Published in final edited form as:
Exp Parasitol. 2013 July ; 134(3): 389–399. doi:10.1016/j.exppara.2013.03.016.

TgMAPK1 is a *Toxoplasma gondii* MAP kinase that hijacks host MKK3 signals to regulate virulence and interferon-γ-mediated nitric oxide production

Michael J. Brumlik[a], **Srilakshmi Pandeswara**[a], **Sara M. Ludwig**[a], **Duane P. Jeansonne**[a], **Michelle R. Lacey**[b], **Kruthi Murthy**[a,c], **Benjamin J. Daniel**[a,b], **Rong-Fu Wang**[d], **Suzanne R. Thibodeaux**[a], **Kristina M. Church**[a], **Vincent Hurez**[a], **Mark J. Kious**[a], **Bin Zhang**[a], **Adebusola Alagbala**[d], **Xiaojun Xia**[d], and **Tyler J. Curiel**[a]

[a]The Cancer Therapy and Research Center/Adult Cancer Program, and the Institute for Drug Development, STRF/8403 Floyd Curl Drive MS 8252/University of Texas Health Science Center, San Antonio, TX 78229, USA

[b]Tulane University, Department of Mathematics, 6823 St. Charles Avenue, New Orleans, LA 70118, USA

[c]Department of Microbiology and Immunology, Graduate School of Biomedical Science, University of Texas Health Science Center at San Antonio, 7703 Floyd Curl Drive, San Antonio, TX 78229, USA

[d]Center for Cell and Gene Therapy and Department of Pathology and Immunology, Baylor College of Medicine, Houston, TX 77030, USA

Abstract

The parasite *Toxoplasma gondii* controls tissue-specific nitric oxide (NO), thereby augmenting virulence and immunopathology through poorly-understood mechanisms. We now identify TgMAPK1, a *Toxoplasma* mitogen-activated protein kinase (MAPK), as a virulence factor regulating tissue-specific parasite burden by manipulating host interferon (IFN)-γ-mediated inducible nitric oxide synthase (iNOS). *Toxoplasma* with reduced TgMAPK1 expression (TgMAPK1^{lo}) demonstrated that TgMAPK1 facilitates IFN-γ-driven p38 MAPK activation, reducing IFN-γ-generated NO in an MKK3-dependent manner, blunting IFN-γ-mediated parasite control. TgMAPK1^{lo} infection in wild type mice produced ≥ten-fold lower parasite burden versus control parasites with normal TgMAPK1 expression (TgMAPK1^{con}). Reduced parasite burdens persisted in IFN-γ KO mice, but equalized in normally iNOS-replete organs from iNOS KO mice. Parasite MAPKs are far less studied than other parasite kinases, but deserve additional attention as targets for immunotherapy and drug discovery.

*Corresponding author address: SA Scientific, Ltd., 4919 Golden Quail, San Antonio, TX 78240, USA. Tel: +1 210 699-8800 michael.brumlik@sascientific.com (M. Brumlik). .

Keywords

iNOS; MAPK; *Toxoplasma gondii*; virulence

1. Introduction

T. gondii is an obligate intracellular protozoan parasite causing life-threatening infections in immunocompromised hosts (Israelski and Remington, 1993). A key host factor controlling anti-*Toxoplasma* immunity is IFN-γ (Denkers, 1999, Suzuki et al., 1988), which mediates anti-parasitic effects through iNOS (Adams et al., 1990), indoleamine 2,3-dioxygenase (Fujigaki et al., 2003), and iGTP (Halonen et al., 2001), among other mechanisms. Few genes subverting these important host immune defenses are known in *Toxoplasma* or other parasites.

MAPKs govern distinct cellular processes in all eukaryotes (Martin-Blanco, 2000), including protozoan parasites (Lacey et al., 2007). We recently identified a *T. gondii* stress-response MAPK designated TgMAPK1 (Brumlik et al., 2004). *T. gondii* inhibits IFN-γ-mediated inducible NO synthase (iNOS) and NO generation (Luder et al., 2003, Rozenfeld et al., 2005, Seabra et al., 2002). We undertook studies testing the hypothesis that TgMAPK1 regulates parasite sensitivity to IFN-γ-mediated defenses.

We show here that TgMAPK1 significantly alters IFN-γ-mediated control of *Toxoplasma* tachyzoite proliferation by manipulating IFN-γ-mediated iNOS and NO generation. TgMAPK1 facilitates IFN-γ-mediated p38 MAPK activation in a MAPK kinase (MKK)3-dependent manner, inhibiting IFN-γ-mediated iNOS expression in iNOS-replete tissues, a novel mechanism to reduce NO. IFN-γ is also a major defense against other medically important intracellular pathogens, including viruses, bacteria and other parasites (Shtrichman and Samuel, 2001). Thus, understanding these strategies against this major immune mediator has wide application. *Toxoplasma* belongs to the phylum Apicomplexa, also comprising agents of babesiosis, cryptosporidiosis and malaria. Therefore, discoveries in *Toxoplasma* can also relate to their immunopathogenesis as well (Kim and Weiss, 2004).

2. Materials and Methods

2.1 Parasites

Parasites were maintained in culture as described elsewhere (Wei et al., 2002). PruΔHXGPRT tachyzoites were from Dr. Laura Knoll (University of Wisconsin Medical School). Dr. David Roos (University of Pennsylvania) provided plasmid pMiniHXGPRT (Donald et al., 1996), into which *tgMAPK1* from plasmid pT7-TgMAPK1 (Brumlik et al., 2004) was cloned in both the sense or antisense orientation. Both resulting plasmids were completely digested with *Sma*I and partially digested with *Eco*RI, deleting all *tgMAPK1* DNA except for the region encompassing the translational initiation site (Seeber, 1997) and the first 17 codons of the coding region (Fig. 1). Recombinant PruΔHXGPRT tachyzoites were then stably transfected with linearized sense and antisense plasmids (Striepen and Soldati, 2007) and both types of clones were isolated by limiting dilution into microtiter

plates. These clones differ in only one critical respect. Antisense knockdown TgMAPK1^{lo} clones express a small transcript that is complementary to approximately 65 nucleotides of the TgMAPK1 transcript (shown by the solid black arrow or box in Fig. 1), and thus is capable of forming double stranded RNA across the region involved in the initiation of translation. In contrast, the sense TgMAPK1^{con} clones express a small control RNA arising from the same DNA sequence, but in this case the DNA is in the opposite orientation in front of the *TUB1* promoter and thus will not hybridize to the TgMAPK1 transcript, thus serving as a control. For certain experiments, TgMAPK1^{con} and TgMAPK1^{lo} clones were additionally stably transfected with plasmid ptubYFP-YFP/sagCAT (Gubbels et al., 2003), which was generously provided by Dr. Boris Striepen (University of Georgia). Genomic DNA was isolated from recombinant and parental *T. gondii* strains as described elsewhere (Medina-Acosta and Cross, 1993). All genotypes were initially verified by PCR and subsequently confirmed by nucleotide sequencing.

2.2. Cells

Human foreskin fibroblasts, J774A.1 and RAW264.7 were from the American Type Culture Collection. RAW264.7 cells were cultured in RPMI-1640 supplemented with 2 mM glutamine, 10 mM 4-(2-hydroxyethyl)-1-piperazineethanesulfonic acid, 10% heat-inactivated fetal bovine serum (FBS), 100 U/mL penicillin, and 100 μg/mL streptomycin. J774A.1 cells were grown in complete Dulbecco's modified Eagle's medium plus 10% heat-inactivated FBS, 2 mM L-glutamine, 100 U/mL penicillin and 100 μg/mL streptomycin. Mouse bone marrow-derived macrophages were prepared as described (Inaba et al., 1992).

2.3. Mice

Mice were 6 – 8 week old C57BL/6 females. WT, IFN-γ KO and iNOS KO mice were purchased from Jackson Laboratory. *p38*$^{fl/fl}$ mice were provided by Drs. Yibin Wang (UCLA) and Huiping Jiang (Boehringer-Ingelheim), and crossed with syngeneic *LysM-Cre*$^{+}$ mice (Jackson Laboratory). MKK3 KO mice (Lu et al., 1999) were from Dr. Richard Flavell (Yale University). All animal studies were approved by our local Institutional Animal Care and Use Committee.

2.4. In vitro T. gondii proliferation

Macrophages were infected with *T. gondii* 16 h before adding murine IFN-γ (PeproTech). Where indicated, *S*-nitroso-*N*-acetyl-penicillamine was added every 24 h, or cells were treated with either 1 mM N^{G}-monomethyl-L-arginine or 1 mM 1-methyltryptophan (all purchased from Sigma) for 2 h before infection. 1 μCi [^{3}H]uracil (Perkin-Elmer) was added 16 h before harvesting cells and [^{3}H]uracil incorporation was measured by liquid scintillation (Curiel et al., 1993).

2.5. Western Blotting

Cells were lysed prior to adding Laemmli buffer (BioRad). Proteins were separated by sodium dodecyl sulfate polyacrylamide gel electrophoresis, transferred to nitrocellulose, blocked in Tris-buffered saline plus 0.1% tween-20 and 5% skim milk and incubated with a 1:1000 dilution of rabbit anti-TgMAPK1 (Lampire Biologicals), mouse anti-*T. gondii* β-

tubulin (gift of Dr. David Sibley, Washington University), rabbit anti-p38 MAPK, anti-phospho-p38 MAPK (all from Cell Signaling), or rabbit anti-mouse iNOS (Santa Cruz Biotechnology) antibodies. Anti-mouse α-tubulin antibody (Sigma) was used at 1:2000. Proteins were detected by enhanced chemiluminescence.

2.6. Serum cytokines

Mouse singleplex antibody beads (Biosource International) were used to detect serum cytokines by Luminex in triplicate according to manufacturer specifications.

2.7. NO production

NO in culture supernatants was measured with Griess reagent (Promega) according to manufacturer specifications.

2.8. Quantitative real-time PCR (qPCR)

Total mouse and *T. gondii* genomic DNA was purified using a DNeasy Blood and Tissue Kit (QIAGEN). The *T. gondii*-specific repeat element *B1* was amplified with 5′-GGAACTGCATCCGTTCATGAG-3′ (*B1* forward) and 5′-TCTTTAAAGCGTTCGTGGTC-3′ (*B1* reverse). *T. gondii* tissue burden was normalized against the mouse genomic hypoxanthine phosphoribosyltransferase 1 (*HPRT1*) gene using 5′-TCATTATGCCGAGGATTTGG-3′ (*HPRT1* forward) and 5′-CACATGCCTCTCCTCTCTCTC-3′ (*HPRT1* reverse) primers. Total mouse tissue RNA was isolated using RNeasy kits (QIAGEN), reverse transcribed using mouse Moloney leukemia virus reverse transcriptase (Invitrogen) and oligo$(dT)_{12\text{-}18}$ primers (Invitrogen). *T. gondii HSP70* was evaluated with 5′-TATATATAACATCAACTTCATATTGTTTTC-3′ (*HSP70* forward) and 5′-TTTTTTTTTTTTTGAATTAGGGATTATTCA-3′ (*HSP70* reverse). *T. gondii* gene expression was normalized against *T. gondii GADPH* using 5′-GTATTGGCCGTCTGGTGTTC-3′ (*GADPH* forward) and 5′-TCGCCAAAACCTCCACGTCG-3′ (*GADPH* reverse). Each reaction contained Sybr Green PCR Master Mix (BioRad) and qPCR was performed using MyiQ single color, real-time PCR detection (BioRad). Quantification of both parasite burden and gene expression were determined using the $2^{-\Delta\Delta CT}$ method (Livak and Schmittgen, 2001).

2.9. Statistical analysis

Statistical analysis of continuous variables used Student's two-tailed *t*-test or two-way ANOVA, as indicated. Mouse survival was estimated by the Kaplan-Meier method and compared by log rank test. Linear statistical models were fit to assess parasite burden by qPCR. To account for correlation among spleen, liver and brain parasite burden for groups of mice, mixed-effects methods were employed using the R package "nlme" (Pinheiro et al., 2008) adjusted for variations. *P* values <0.05 were considered significant.

3. Results

3.1. TgMAPK1 regulates parasite tissue burden

T. gondii tachyzoites with either ~ten-fold reduced TgMAPK1 (TgMAPK1^{lo}) or normal levels of TgMAPK1 (control; TgMAPK1^{con}) were generated using plasmids constitutively expressing antisense or sense *tgMAPK1* RNA, respectively, transcribed from the *TUB1* promoter (Fig. 1). Control (TgMAPK1^{con}) tachyzoites expressed TgMAPK1 levels indistinguishable from parental tachyzoites (Fig. 2a). Using real-time RT-PCR, we found that both the TgMAPK1^{con} and TgMAPK1^{lo} expressed the same amount of *tgMAPK1* transcript (not shown), suggesting that the antisense knockdown interferes with the translation of the *tgMAPK1* gene. One hallmark of the TgMAPK1^{lo} phenotype is the fact that these tachyzoites grow at a significantly slower rate in cultured human foreskin fibroblasts compared to either TgMAPK1^{con} or the parental strain from which they were derived (Fig. 2b).

TgMAPK1^{lo}-infected C57BL/6 wild type (WT) mice exhibited approximately ten-fold lower *Toxoplasma* burden in spleen, liver and brain versus TgMAPK1^{con}-infection (Fig. 3a; $P<0.009$ for each organ). IFN-γ is pivotal in controlling *T. gondii* infection (Denkers, 1999, Suzuki et al., 1988). Nonetheless, TgMAPK1^{lo} and TgMAPK1^{con} induced equivalent serum IFN-γ (Fig. 3b; $P=0.154$) and IL-10 (Fig. 3b; $P=0.143$), a negative regulator of IFN-γ and other anti-*Toxoplasma* defenses (Gazzinelli et al., 1996).

3.2. TgMAPK1-mediated differential parasite tissue burden persists in the absence of IFN-γ

We next challenged syngeneic, IFN-γ-deficient IFN-γ KO mice with TgMAPK1^{con} or TgMAPK1^{lo} tachyzoites, which produced significantly higher parasite burdens for both compared to respective infections in WT mice (Fig. 3a; $P<0.001$ for all tissues), consistent with known IFN-γ effects on *T. gondii* replication (Scharton-Kersten et al., 1996) and demonstrating IFN-γ-mediated control of parasite burden *in vivo*. Nonetheless, the approximately ten-fold higher tissue burden in TgMAPK1^{con} versus TgMAPK1^{lo} infection was preserved in all tissues examined (Fig. 3a; $P<0.01$), suggesting that factors besides IFN-γ also regulated TgMAPK1-dependent differential tissue-specific parasite burden.

3.3. IFN-γ differentially regulates TgMAPK1^{lo} versus TgMAPK1^{con} tachyzoite proliferation in vitro

We tested tachyzoite growth in macrophages *in vitro*, as they are important agents of parasite dissemination *in vivo* (Courret et al., 2006). As was seen in human foreskin fibroblasts (Fig. 2b), TgMAPK1^{lo} grew slower than TgMAPK1^{con} in WT mouse bone marrow-derived macrophages (BMDM) (Fig. 4a; $P<0.001$) by [^{3}H]uracil uptake in the absence of IFN-γ. Strikingly, TgMAPK1^{lo} tachyzoite proliferation was reduced by exogenous IFN-γ significantly greater than TgMAPK1^{con} tachyzoites in BMDM (Fig. 4b; $P<0.001$). As IFN-γ effects could be cell or background-specific, we showed differential IFN-γ sensitivity in infected BALB/c J774A.1 (Fig. 4c; left panel; $P<0.001$) and RAW264.7 macrophage cell lines (not shown).

3.4. TgMAPK1-mediated tachyzoite IFN-γ sensitivity is governed by TgMAPK1-regulated IFN-γ-induced iNOS and NO

NO is a major downstream mediator of IFN-γ effects on *Toxoplasma* proliferation (Langermans et al., 1992). In support, the iNOS inhibitor N^G-monomethyl-L-arginine (L-NMMA) equalized IFN-γ-mediated TgMAPK1^{lo} and TgMAPK1^{con} tachyzoite replication inhibition in J774A.1 macrophages (Fig. 4c; middle panel; P=0.552), circumstances where iNOS is highly expressed (Fig. 5a) and NO (Fig. 5b) is produced at significant levels. Equalized tachyzoite proliferation control was largely from reduced IFN-γ-mediated TgMAPK1^{lo} replication control rather than from enhanced TgMAPK1^{con} replication (compare left versus middle panels, Fig. 4c). TgMAPK1^{lo} and TgMAPK1^{con} tachyzoite proliferation *in vitro* (based on β-tubulin expression) inversely correlated with differential IFN-γ-mediated iNOS expression (Fig. 5a) further suggesting NO as a final common regulator of TgMAPK1-dependent tachyzoite IFN-γ sensitivity. We also showed that differential IFN-γ-mediated control of TgMAPK1^{lo} or TgMAPK1^{con} tachyzoite proliferation was abolished in BMDM treated with L-NMMA (Fig. 5c; P=0.552). Together, these data demonstrate that TgMAPK1 regulation of IFN-γ-induced iNOS and NO generation accounts for differential TgMAPK1-dependent IFN-γ-mediated control of tachyzoite proliferation. L-NMMA also enhanced the proliferation of both TgMAPK1^{lo} and TgMAPK1^{con} in macrophages cultured in the absence of IFN-γ (Figs. 3d and 3e; P<0.001 for each), suggesting that IFN-γ-independent NO production below our limits of detection ([NO_2^-] < 1 μM; Fig. 5b) can presumably still inhibit parasite proliferation but does not alter differential TgMAPK1-dependent growth rates (Fig. 4e).

3.5. Indoleamine 2,3-dioxygenase does not contribute to differential TgMAPK1-dependent IFN-γ control of tachyzoite proliferation

Indoleamine 2,3-dioxygenase (IDO) is another IFN-γ-mediated defense against *Toxoplasma* infection. However, the IDO inhibitor 1-methyltryptophan did not abrogate differential IFN-γ-mediated control of TgMAPK1^{lo} versus TgMAPK1^{con} tachyzoite replication in cultured macrophages (Fig. 4c; right panel; P<0.001). Furthermore, in the absence of IFN-γ administration, 1-methyltryptophan increased the proliferation of both TgMAPK1^{lo} and TgMAPK1^{con} in macrophages equivalently (Fig. 4e), suggesting that IDO contributes to controlling parasite replication in the absence of IFN-γ and that TgMAPK1^{lo} and TgMAPK1^{con} are equally IDO-sensitive.

3.6. TgMAPK1 controls IFN-γ-mediated macrophage iNOS expression

IFN-γ induced three-fold higher iNOS in TgMAPK1^{lo} infected versus TgMAPK1^{con} infected BMDM from syngeneic *p38$^{fl/fl}$LysM-Cre$^-$* mice, functionally equivalent to WT C57BL/6 macrophages (Engel et al., 2005) (Fig. 5a). IFN-γ induced significant NO in uninfected RAW264.7 macrophages that was reduced by *Toxoplasma* infection (Fig. 5b; P<0.001) as reported (Luder et al., 2003). TgMAPK1^{con}-infected cells produced less IFN-γ-mediated NO versus TgMAPK1^{lo}-infected cells (Fig. 5b; P<0.001 for both macrophage lines). Together, these data demonstrate that TgMAPK1 suppresses tachyzoite-mediated and/or host IFN-γ-mediated iNOS expression and NO production.

3.7. TgMAPK1 does not alter tachyzoite NO sensitivity

At first glance, TgMAPK1^{lo} proliferation appeared more sensitive to the NO donor *S*-nitroso-*N*-acetylpenicillamine (SNAP) versus TgMAPK1^{con} infection in WT BMDM (Fig. 6a). However, when tachyzoite proliferation was plotted versus total measured nitrite concentration, TgMAPK1^{lo} and TgMAPK1^{con} were equally NO-sensitive (Fig. 6b), consistent with the fact that endogenous NO production in TgMAPK1^{lo}-infected macrophages was higher compared to TgMAPK1^{con} infection (Fig. 5b) even in the absence of exogenous IFN-γ.

3.8. Parasite burden equalizes in spleens and livers of iNOS-deficient mice

Because IFN-γ-mediated iNOS generation controls *T. gondii* infection (Gazzinelli et al., 1993, Luder et al., 2003), we tested parasite burden in infected, syngeneic, iNOS-deficient iNOS KO mice. Consistent with earlier reports (Khan et al., 1997), TgMAPK1^{con} parasite burden was significantly higher in spleen and liver in iNOS KO versus WT mice (Fig. 6c; $P<0.001$ for each organ). TgMAPK1^{lo} parasite burden was also significantly higher in livers and spleens of iNOS KO versus WT mice (Fig. 6c; $P<0.001$ for each organ), demonstrating iNOS-mediated control of TgMAPK1^{con} and TgMAPK1^{lo} tachyzoites in these organs. Remarkably, yet supporting our hypothesis, thêten-fold decreased parasite burden in WT mice infected with TgMAPK1^{lo} versus TgMAPK1^{con} equalized in spleens and livers of iNOS KO mice (Fig. 6c; $P=0.919$ and 0.797, respectively), in which WT organs are iNOS-replete (Fujigaki et al., 2002), suggesting that local iNOS is a key regulator of local parasite burden.

By contrast, but further supporting our hypothesis, parasite burden in iNOS KO mice did not equalize in brain, which expresses little iNOS (Fujigaki et al., 2002), and differential TgMAPK1^{lo} versus TgMAPK1^{con} brain burden was essentially equivalent in WT versus iNOS KO mice (Fig. 6c; $P=0.470$). Results are consistent with a relatively insignificant role for brain iNOS in controlling local *Toxoplasma* burden as previously reported (Fujigaki et al., 2002, Sato et al., 1995), and suggest that brain parasite burden is regulated distinctly (Martens et al., 2005) in a TgMAPK1-dependent, but iNOS-independent fashion. Because NO production in WT mice was below detection limits, local NO production could not be further evaluated.

Differential IFN-γ-mediated proliferation control of TgMAPK1^{lo} versus TgMAPK1^{con} was abrogated in iNOS KO BMDM (Fig. 7a; $P=0.095$), further supporting critical iNOS contributions to IFN-γ-mediated tachyzoite proliferation control, and its dependence on TgMAPK1. Together with parasite burden results from liver and spleen, these data further demonstrate that differential *in vivo* parasite burden is not simply a reflection of differential basal tachyzoite growth rates but accord with tissue-specific TgMAPK1-mediated and NO-dependent control of parasite burden. Nonetheless, differential TgMAPK1-dependent tachyzoite growth rates remained in iNOS KO BMDM (Fig. 7b; $P<0.001$) suggesting iNOS-independent mechanisms for differential growth control, and consistent with differential tissue burden differences in iNOS KO brain (Fig. 6c).

3.9. TgMAPK1-mediated tachyzoite IFN-γ sensitivity regulation is p38 MAPK-dependent

The *Toxoplasma* virulence factor heat shock protein (HSP) 70 is the only parasite protein previously known to regulate host iNOS (Dobbin et al., 2002), but *HSP70* mRNA was equivalent in tachyzoites in WT BMDM infected with TgMAPK1^{lo} or TgMAPK1^{con} (Fig. 7c; P=0.431), suggesting a novel TgMAPK1-dependent parasite-mediated iNOS control mechanism. On the other hand, host p38 MAPK is a stress-response protein affected by *T. gondii* (Kim et al., 2005) and regulating iNOS (Chen et al., 1999). TgMAPK1 facilitated IFN-γ-mediated p38 MAPK activation in infected cells as IFN-γ activated p38 MAPK significantly better in TgMAPK1^{con} versus TgMAPK1^{lo}-infected BMDM from *p38$^{fl/fl}$ LysM-Cre^{-}* mice (with WT p38 MAPK levels) (Fig. 5a). In support of a p38 MAPK-dependent mechanism, differential IFN-γ-mediated control of tachyzoite growth (based on β-tubulin expression) was abolished in *p38$^{fl/fl}$ LysM-Cre^{+}* BMDM lacking p38 MAPK (Fig. 5a).

3.10. TgMAPK1-dependent p38 MAPK-dependent NO production regulates parasite IFN-γ sensitivity

We suspected that p38 MAPK-dependent NO ultimately mediated IFN-γ effects. By contrast to p38 MAPK sufficient BMDM, IFN-γ elicited equal iNOS in TgMAPK1^{lo}- or TgMAPK1^{con}-infected p38-deficient BMDM (Fig. 5a), consistent with the requirement for host p38 MAPK activation to suppress iNOS during infection. Also consistent with NO production as the final mediator of growth suppression in iNOS-replete tissues, differential IFN-γ-mediated TgMAPK1^{con} and TgMAPK1^{lo} tachyzoite proliferation control was abolished in L-NMMA-treated p38 MAPK-sufficient and -deficient BMDM (Fig. 5c). Together, these data are consistent with TgMAPK1 facilitating IFN-γ-driven host cell p38 MAPK activation, thereby reducing IFN-γ-mediated iNOS-dependent NO that ultimately regulates parasite proliferation *in vitro* and parasite burden *in vivo* in iNOS-replete tissues.

3.11. TgMAPK1-dependent IFN-γ-driven p38 MAPK activation is MKK3-dependent

MKK3 is a key upstream activator of p38 MAPK (Lu et al., 1999). Differential IFN-γ-mediated p38 MAPK activation in infected BMDM (Fig. 5a) was abolished in infected syngeneic, MKK3-deficient MKK3 KO BMDM (Fig. 7d), demonstrating that MKK3 regulates IFN-γ-driven p38 MAPK activation in infected WT BMDM in a TgMAPK1-dependent fashion. Moreover, the increased iNOS in TgMAPK1^{lo}-infected WT BMDM versus TgMAPK1^{con} infection (Fig. 5a) was abrogated in MKK3 KO BMDM (Fig. 7d). Differential IFN-γ-mediated TgMAPK1^{lo} versus TgMAPK1^{con} tachyzoite proliferation control in WT BMDM (Figs. 3b and 4a) was likewise abrogated in MKK3 KO BMDM (Fig. 7e; P=0.933). Together, these data demonstrate that TgMAPK1 regulation of IFN-γ-dependent p38 MAPK activation, host iNOS production and tachyzoite growth control are all MKK3-dependent. Nonetheless, differential growth of TgMAPK1^{lo} versus TgMAPK1^{con} tachyzoites persisted in MKK3 KO macrophages (Fig. 7f; P<0.001).

3.12 Reduced TgMAPK1 expression attenuates T. gondii virulence in an IFN-γ, iNOS and MKK3-dependent manner

To assess TgMAPK1 virulence effects we infected WT mice with 50,000 PruΔHXGPRT (not shown) or TgMAPK1^{con} tachyzoites (Fig. 8a), which was invariably fatal one week post-infection. By contrast, half the mice infected with 50,000 TgMAPK1^{lo} tachyzoites survived up to 6 additional days (Fig. 8a; $P<0.001$), demonstrating that TgMAPK1 is a virulence factor. Even with a lower 10,000 tachyzoite challenge, reduced virulence of TgMAPK1^{lo} tachyzoites was abrogated in IFN-γ KO mice (Fig. 8b; $P=0.858$) demonstrating IFN-γ contributions to TgMAPK1-dependent virulence. iNOS KO mice challenged with 10,000 TgMAPK1^{lo} or TgMAPK1^{con} tachyzoites survived equally (Fig. 8c; $P=0.350$), demonstrating that TgMAPK1-dependent virulence is also iNOS-dependent. Because p38 MAPK null mice are embryonic lethal (Lu et al., 1999) we challenged MKK3 KO mice with 10,000 TgMAPK1^{lo} or TgMAPK1^{con} tachyzoites and found that the virulence difference was eliminated (Fig. 8d; $P=0.632$), demonstrating the MKK3-dependence of TgMAPK1-mediated virulence, consistent with a role for TgMAPK1-mediated virulence through MKK3-dependent p38 MAPK activation.

4. Discussion

Although parasitic infection causes significant world-wide health and economic burdens, understanding the immunopathology of parasitic infections lags that of other pathogens. Host signaling pathway subversion to evade immunity is a significant strategy employed by successful pathogens including parasites such as *T. gondii*, among the most successful of pathogens as evidenced by its extremely varied host range, which includes essentially all mammals and many birds (Elmore et al., 2010). Although *T. gondii* subversion of host cell signaling is well-described (Blader and Saeij, 2009, Boothroyd and Dubremetz, 2008), few specific pathogen factors or mechanisms affecting virulence and host immunity are known.

We now identify the *T. gondii* MAPK TgMAPK1 as an important manipulator of host immunity and regulator of parasite burden and virulence. MAPKs regulate multiple downstream pathways with diverse effects (Kültz, 1998). The functions of protozoan MAPKs from *Leishmania, Plasmodium*, and *Trypanosoma* have been partially elucidated, demonstrating that they modulate parasite virulence, stress-responses, differentiation and proliferation [reviewed in reference (Brumlik et al., 2011)].

We previously demonstrated that TgMAPK1 mediates osmotic stress responses (Brumlik et al., 2004). Here we studied effects on key host immune defenses and parasite burden. TgMAPK1 deficiency reduced tissue parasite burden. IFN-γ is critical in defense against *T. gondii* (Suzuki et al., 1988) and control of parasite burden (Scharton-Kersten et al., 1996), yet TgMAPK1 did not affect serum IFN-γ during infection, prompting us to investigate TgMAPK1-dependent tachyzoite IFN-γ sensitivity as a basis for differential parasite burden.

TgMAPK1 sufficient tachyzoites impaired IFN-γ-mediated growth control *in vitro* suggesting a mechanism for differential *in vivo* parasite burden. Burdens of both TgMAPK1^{con} and TgMAPK1^{lo} tachyzoites increased significantly during infection in IFN-γ KO mice but remained ten-fold different between TgMAPK1^{con} and TgMAPK1^{lo},

demonstrating that IFN-γ can control tachyzoite proliferation even when TgMAPK1 is low, but that IFN-γ-independent factors also regulate *T. gondii* burden. IDO is a key mediator of IFN-γ anti-pathogen effects, but we found no evidence that it contributes to differential tachyzoite growth control when IFN-γ signals are sufficient. However, tachyzoites were sensitive to IDO-mediated growth control irrespective of the level of TgMAPK1 expression. Thus, IDO could help regulate *Toxoplasma* burden when local IFN-γ is limiting.

The other major downstream mediator of IFN-γ is NO. *In vitro*, we demonstrated that TgMAPK1 controlled IFN-γ-mediated iNOS expression and NO production, suggesting that blocking IFN-γ-mediated NO could be a mechanism for TgMAPK1-dependent regulation of IFN-γ-mediated tachyzoite control, which we confirmed by showing loss of differential IFN-γ anti-proliferative effects *in vitro* when iNOS enzymatic activity was inhibited. Further, differential IFN-γ-mediated control of tachyzoite replication regulated by TgMAPK1 was specifically through control of NO concentration, as TgMAPK1 did not significantly affect tachyzoite NO sensitivity. Pathogens such as *Leishmania* are known to regulate NO (Wilkins-Rodriguez et al., 2010), demonstrating the importance of controlling host NO by other important pathogens. These data suggest that pharmacologic control of local NO could be a useful approach to anti-parasite drug development.

To test *in vivo* effects of TgMAPK1-dependent iNOS manipulation, we showed that differential parasite burdens between TgMAPK1^{lo} and TgMAPK1^{con} equalized in iNOS KO mice in tissues normally iNOS-replete. These data support the concept that local parasite control is through TgMAPK1-dependent NO production independent of basal parasite replication rates. In further support, TgMAPK1-dependent differential parasite burdens did not equalize in iNOS KO mouse brains, where parasite burdens were essentially unchanged versus WT brains, consistent with prior reports that iNOS is not a significant host regulator of parasite burden in brain (Fujigaki et al., 2002, Sato et al., 1995). We detected little *IDO* transcript in WT brain during infection (not shown). Lack of NO- and IDO-regulated control of *T. gondii* in the central nervous system likely contributes to its predilection to induce brain pathology (Luft and Remington, 1992). The IFN-γ-independent mechanism for iNOS induction and NO-independent mechanisms of tachyzoite control in iNOS-replete tissues remain incompletely defined. Our work further establishes TgMAPK1 as a parasite factor controlling brain tissue burden although the corresponding host factor(s) controlling brain tissue parasite burden remain unknown.

To understand how TgMAPK1 manipulated iNOS, we first showed that TgMAPK1 did not affect *T. gondii HSP70* expression, the sole *Toxoplasma* virulence gene reported to manipulate host iNOS (Dobbin et al., 2002). Instead, we demonstrated a novel mechanism of iNOS regulation through parasite hijacking of host p38 MAPK signaling: TgMAPK1 augments host cell p38 MAPK activation, thereby limiting host iNOS production. In support of this concept, infection with either TgMAPK1^{con} or TgMAPK1^{lo} tachyzoites in macrophages lacking p38 MAPK generated equivalent elevated levels of iNOS, circumstances where TgMAPK1-dependent differential parasite susceptibility to IFN-γ-mediated proliferation suppression was abolished. Our data also demonstrate an unexpected and previously undefined requirement for MKK3-dependent p38 MAPK activation that inhibits IFN-γ-induced iNOS, thereby limiting local NO. Macrophages exposed to IFN-γ

before *T. gondii* infection activate p38 MAPK in a tumor necrosis factor receptor associated factor-6-dependent manner (Mason et al., 2004) in which MKK3 activate p38 MAPK (Landstrom, 2010). We clearly demonstrate that MKK3 signals are sufficient for TgMAPK1-dependent IFN-γ, iNOS and virulence effects. Specifically how TgMAPK1 hijacks MKK3 signaling is unknown, and could involve direct interactions with parasite proteins injected during infection (Saeij et al., 2006), direct interactions between the parasitophorus vacuole and host cell, or indirect consequences of other parasite or host factors as recently reviewed (Blader and Saeij, 2009).

Our work finally establishes TgMAPK1 as a novel *T. gondii* virulence factor that is iNOS, IFN-γ and MKK3-dependent. Because virulence was equivalent irrespective of TgMAPK1 expression in IFN-γ KO mice where TgMAPK1^{lo} burden remained ten-fold below TgMAPK1^{con} burden, TgMAPK1-dependent virulence is unlikely due solely to differential parasite burden. We are currently investigating additional MKK3 and p38 MAPK-dependent immune mechanisms as possibilities.

Our data demonstrate that parasite MAPK gene products can have significant immunopathologic and virulence effects that merit additional study to help understand their immunopathogenesis better and to novel drug discovery targets.

Acknowledgments

This work was supported by the National Institutes of Health grant AI060424 and a Johnson and Johnson Focused Giving Award (both to T.J.C.).

References

Adams LB, Hibbs JB Jr. Taintor RR, Krahenbuhl JL. Microbiostatic effect of murine-activated macrophages for *Toxoplasma gondii*. Role for synthesis of inorganic nitrogen oxides from L-arginine. J Immunol. 1990; 144:2725–2729. [PubMed: 2319133]

Blader IJ, Saeij JP. Communication between *Toxoplasma gondii* and its host: impact on parasite growth, development, immune evasion, and virulence. Apmis. 2009; 117:458–476. [PubMed: 19400868]

Boothroyd JC, Dubremetz JF. Kiss and spit: the dual roles of *Toxoplasma* rhoptries. Nat Rev Microbiol. 2008; 6:79–88. [PubMed: 18059289]

Brumlik MJ, Pandeswara S, Ludwig SM, Murthi K, Curiel TJ. Parasite mitogen-activated protein kinases as drug discovery targets to treat human protozoan pathogens. Journal of Signal Transduction. 2011; 2011; 16pp

Brumlik MJ, Wei S, Finstad K, Nesbit J, Hyman LE, Lacey M, Burow ME, Curiel TJ. Identification of a novel mitogen-activated protein kinase in *Toxoplasma gondii*. Int J Parasitol. 2004; 34:1245–1254. [PubMed: 15491587]

Chen C, Chen YH, Lin WW. Involvement of p38 mitogen-activated protein kinase in lipopolysaccharide-induced iNOS and COX-2 expression in J774 macrophages. Immunology. 1999; 97:124–129. [PubMed: 10447723]

Courret N, Darche S, Sonigo P, Milon G, Buzoni-Gatel D, Tardieux I. CD11c- and CD11b-expressing mouse leukocytes transport single *Toxoplasma gondii* tachyzoites to the brain. Blood. 2006; 107:309–316. [PubMed: 16051744]

Curiel TJ, Krug EC, Purner MB, Poignard P, Berens RL. Cloned human CD4+ cytotoxic T lymphocytes specific for *Toxoplasma gondii* lyse tachyzoite-infected target cells. J Immunol. 1993; 151:2024–2031. [PubMed: 8102155]

Denkers EY. T lymphocyte-dependent effector mechanisms of immunity to *Toxoplasma gondii*. Microbes Infect. 1999; 1:699–708. [PubMed: 10611747]

Dobbin CA, Smith NC, Johnson AM. Heat shock protein 70 is a potential virulence factor in murine *Toxoplasma* infection via immunomodulation of host NF-kappa B and nitric oxide. J Immunol. 2002; 169:958–965. [PubMed: 12097402]

Donald RG, Carter D, Ullman B, Roos DS. Insertional tagging, cloning, and expression of the *Toxoplasma gondii* hypoxanthine-xanthine-guanine phosphoribosyltransferase gene. Use as a selectable marker for stable transformation. J Biol Chem. 1996; 271:14010–14019. [PubMed: 8662859]

Elmore SA, Jones JL, Conrad PA, Patton S, Lindsay DS, Dubey JP. *Toxoplasma gondii*: epidemiology, feline clinical aspects, and prevention. Trends Parasitol. 2010; 26:190–196. [PubMed: 20202907]

Engel FB, Schebesta M, Duong MT, Lu G, Ren S, Madwed JB, Jiang H, Wang Y, Keating MT. p38 MAP kinase inhibition enables proliferation of adult mammalian cardiomyocytes. Genes Dev. 2005; 19:1175–1187. [PubMed: 15870258]

Fujigaki S, Saito K, Takemura M, Maekawa N, Yamada Y, Wada H, Seishima M. L-tryptophan-L-kynurenine pathway metabolism accelerated by *Toxoplasma gondii* infection is abolished in gamma interferon-gene-deficient mice: cross-regulation between inducible nitric oxide synthase and indoleamine-2,3-dioxygenase. Infect Immun. 2002; 70:779–786. [PubMed: 11796611]

Fujigaki S, Takemura M, Hamakawa H, Seishima M, Saito K. The mechanism of interferon-gamma induced anti *Toxoplasma gondii* by indoleamine 2,3-dioxygenase and/or inducible nitric oxide synthase vary among tissues. Adv Exp Med Biol. 2003; 527:97–103. [PubMed: 15206721]

Gazzinelli RT, Amichay D, Sharton-Kersten T, Grunwald E, Farber JM, Sher A. Role of macrophage-derived cytokines in the induction and regulation of cell-mediated immunity to *Toxoplasma gondii*. Curr Top Microbiol Immunol. 1996; 219:127–139. [PubMed: 8791695]

Gazzinelli RT, Eltoum I, Wynn TA, Sher A. Acute cerebral toxoplasmosis is induced by in vivo neutralization of TNF-alpha and correlates with the down-regulated expression of inducible nitric oxide synthase and other markers of macrophage activation. Journal of Immunology. 1993; 151:3672–3681.

Gubbels MJ, Li C, Striepen B. High-throughput growth assay for *Toxoplasma gondii* using yellow fluorescent protein. Antimicrob Agents Chemother. 2003; 47:309–316. [PubMed: 12499207]

Halonen SK, Taylor GA, Weiss LM. Gamma interferon-induced inhibition of *Toxoplasma gondii* in astrocytes is mediated by IGTP. Infect Immun. 2001; 69:5573–5576. [PubMed: 11500431]

Inaba K, Inaba M, Romani N, Aya H, Deguchi M, Ikehara S, Muramatsu S, Steinman RM. Generation of large numbers of dendritic cells from mouse bone marrow cultures supplemented with granulocyte/macrophage colony-stimulating factor. J Exp Med. 1992; 176:1693–1702. [PubMed: 1460426]

Israelski DM, Remington JS. Toxoplasmosis in the non-AIDS immunocompromised host. Curr Clin Top Infect Dis. 1993; 13:322–356. [PubMed: 8397917]

Khan IA, Schwartzman JD, Matsuura T, Kasper LH. A dichotomous role for nitric oxide during acute *Toxoplasma gondii* infection in mice. Proceedings of the National Academy of Sciences of the United States of America. 1997; 94:13955–13960. [PubMed: 9391134]

Kim K, Weiss LM. *Toxoplasma gondii*: the model apicomplexan. Int J Parasitol. 2004; 34:423–432. [PubMed: 15003501]

Kim L, Del Rio L, Butcher BA, Mogensen TH, Paludan SR, Flavell RA, Denkers EY. p38 MAPK autophosphorylation drives macrophage IL-12 production during intracellular infection. Journal of Immunology. 2005; 174:4178–4184.

Kültz D. Phylogenetic and functional classification of mitogen- and stress-activated protein kinases. J Mol Evol. 1998; 46:571–588. [PubMed: 9545468]

Lacey MR, Brumlik MJ, Yenni RE, Burow ME, Curiel TJ. *Toxoplasma gondii* expresses two mitogen-activated protein kinase genes that represent distinct protozoan subfamilies. J Mol Evol. 2007; 64:4–14. [PubMed: 17160647]

Landstrom M. The TAK1-TRAF6 signalling pathway. Int J Biochem Cell Biol. 2010; 42:585–589. [PubMed: 20060931]

Langermans JA, Van der Hulst ME, Nibbering PH, Hiemstra PS, Fransen L, Van Furth R. IFN-gamma-induced L-arginine-dependent toxoplasmastatic activity in murine peritoneal macrophages is mediated by endogenous tumor necrosis factor-alpha. J Immunol. 1992; 148:568–574. [PubMed: 1729374]

Livak KJ, Schmittgen TD. Analysis of relative gene expression data using real-time quantitative PCR and the 2(-Delta Delta C(T)) Method. Methods. 2001; 25:402–408. [PubMed: 11846609]

Lu HT, Yang DD, Wysk M, Gatti E, Mellman I, Davis RJ, Flavell RA. Defective IL-12 production in mitogen-activated protein (MAP) kinase kinase 3 (Mkk3)-deficient mice. Embo J. 1999; 18:1845–1857. [PubMed: 10202148]

Luder CG, Algner M, Lang C, Bleicher N, Gross U. Reduced expression of the inducible nitric oxide synthase after infection with *Toxoplasma gondii* facilitates parasite replication in activated murine macrophages. Int J Parasitol. 2003; 33:833–844. [PubMed: 12865083]

Luft BJ, Remington JS. Toxoplasmic encephalitis in AIDS. Clin Infect Dis. 1992; 15:211–222. [PubMed: 1520757]

Martens S, Parvanova I, Zerrahn J, Griffiths G, Schell G, Reichmann G, Howard JC. Disruption of *Toxoplasma gondii* parasitophorous vacuoles by the mouse p47-resistance GTPases. PLoS Pathog. 2005; 1:e24. [PubMed: 16304607]

Martin-Blanco E. p38 MAPK signalling cascades: ancient roles and new functions. Bioessays. Bioessays. 2000; 22:637–645. [PubMed: 10878576]

Mason NJ, Fiore J, Kobayashi T, Masek KS, Choi Y, Hunter CA. TRAF6-dependent mitogen-activated protein kinase activation differentially regulates the production of interleukin-12 by macrophages in response to *Toxoplasma gondii*. Infect Immun. 2004; 72:5662–5667. [PubMed: 15385464]

Medina-Acosta E, Cross GA. Rapid isolation of DNA from trypanosomatid protozoa using a simple 'mini-prep' procedure. Mol Biochem Parasitol. 1993; 59:327–329. [PubMed: 8341329]

Pinheiro, J.; Bates, D.; DebRoy, S.; Sarkar, D.; Team, RC. R package version 3. 2008. nlme: Linear and Nonlinear Mixed Effects Models; p. 1-89.

Rozenfeld C, Martinez R, Seabra S, Sant'anna C, Goncalves JG, Bozza M, Moura-Neto V, De Souza W. *Toxoplasma gondii* prevents neuron degeneration by interferon-gamma-activated microglia in a mechanism involving inhibition of inducible nitric oxide synthase and transforming growth factor-beta1 production by infected microglia. Am J Pathol. 2005; 167:1021–1031. [PubMed: 16192637]

Saeij JP, Boyle JP, Coller S, Taylor S, Sibley LD, Brooke-Powell ET, Ajioka JW, Boothroyd JC. Polymorphic secreted kinases are key virulence factors in toxoplasmosis. Science. 2006; 314:1780–1783. [PubMed: 17170306]

Sato K, Miyakawa K, Takeya M, Hattori R, Yui Y, Sunamoto M, Ichimori Y, Ushio Y, Takahashi K. Immunohistochemical expression of inducible nitric oxide synthase (iNOS) in reversible endotoxic shock studied by a novel monoclonal antibody against rat iNOS. J Leukoc Biol. 1995; 57:36–44. [PubMed: 7530282]

Scharton-Kersten TM, Wynn TA, Denkers EY, Bala S, Grunvald E, Hieny S, Gazzinelli RT, Sher A. In the absence of endogenous IFN-gamma, mice develop unimpaired IL-12 responses to *Toxoplasma gondii* while failing to control acute infection. J Immunol. 1996; 157:4045–4054. [PubMed: 8892638]

Seabra SH, de Souza W, DaMatta RA. *Toxoplasma gondii* partially inhibits nitric oxide production of activated murine macrophages. Exp Parasitol. 2002; 100:62–70. [PubMed: 11971655]

Seeber F. Consensus sequence of translational initiation sites from *Toxoplasma gondii* genes. Parasitol Res. 1997; 83:309–311. [PubMed: 9089733]

Shtrichman R, Samuel CE. The role of gamma interferon in antimicrobial immunity. Curr Opin Microbiol. 2001; 4:251–259. [PubMed: 11378475]

Striepen, B.; Soldati, D. Genetic manipulation of *Toxoplasma gondii*. Elsevier; 2007.

Suzuki Y, Orellana MA, Schreiber RD, Remington JS. Interferon-gamma: the major mediator of resistance against *Toxoplasma gondii*. Science. 1988; 240:516–518. [PubMed: 3128869]

Wei S, Marches F, Daniel B, Sonda S, Heidenreich K, Curiel T. Pyridinylimidazole p38 mitogen-activated protein kinase inhibitors block intracellular *Toxoplasma gondii* replication. Int J Parasitol. 2002; 32:969–977. [PubMed: 12076626]

Wilkins-Rodriguez AA, Escalona-Montano AR, Aguirre-Garcia M, Becker I, Gutierrez-Kobeh L. Regulation of the expression of nitric oxide synthase by *Leishmania mexicana* amastigotes in murine dendritic cells. Exp Parasitol. 2010; 126:426–434. [PubMed: 20659463]

- TgMAPK1 is a *Toxoplasma gondii* mitogen-activated protein kinase (MAPK).
- It affects parasite proliferation in an IFN-γ, iNOS and MKK3-dependent manner.
- Parasite tissue burden is regulated by TgMAPK1 expression in iNOS-replete tissues.
- Thus TgMAPK1 ultimately affects virulence by manipulating host IFN-γ-mediated iNOS.

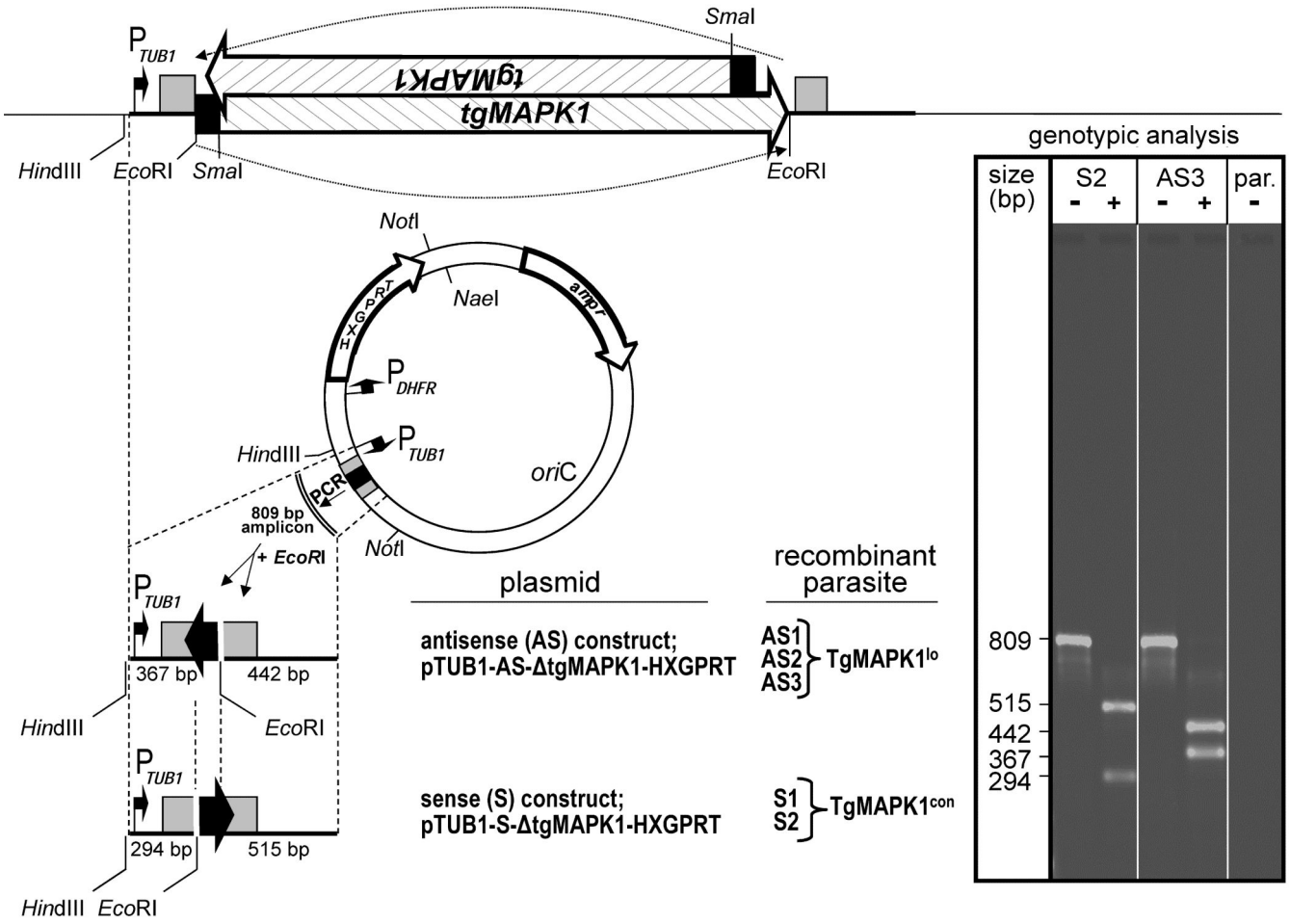

Fig. 1.

Construction of TgMAPK1^{lo} tachyzoites. Both sense (control) and antisense knockdown plasmids were constructed from pMiniHXGPRT and were stably transfected into parental (par) *T. gondii* Prugniaud strain deleted for *HXGPRT* (hypoxanthine-guanine phosphoribosyltransferase; PruΔHXGPRT). Filled black arrows indicate DNA orientation. The *T. gondii* α-tubulin (*TUB1*) and dihydrofolate reductase (*DHFR*) promoters are indicated by arrows with right angles. 5′ (*TUB1*) and 3′ (*SAG1*) untranslated regions are indicated by gray boxes. Clonally-derived sense (TgMAPK1^{con}; S1 and S2) and antisense (TgMAPK1^{lo}; AS1 – AS3) recombinant parasites were initially confirmed by genotypic analysis following PCR amplification of the 809 bp amplicon. These reactions were either digested with *Eco*RI (+) or remained undigested (−) prior to electrophoresis. DNA size is shown in base pairs (bp). Genotypes were ultimately verified by nucleotide sequencing (not shown). Genotype profiles of the parental strain (par.), one representative sense (S2) and antisense (AS3) clone are shown in the ethidium bromide stained gel shown in the inset.

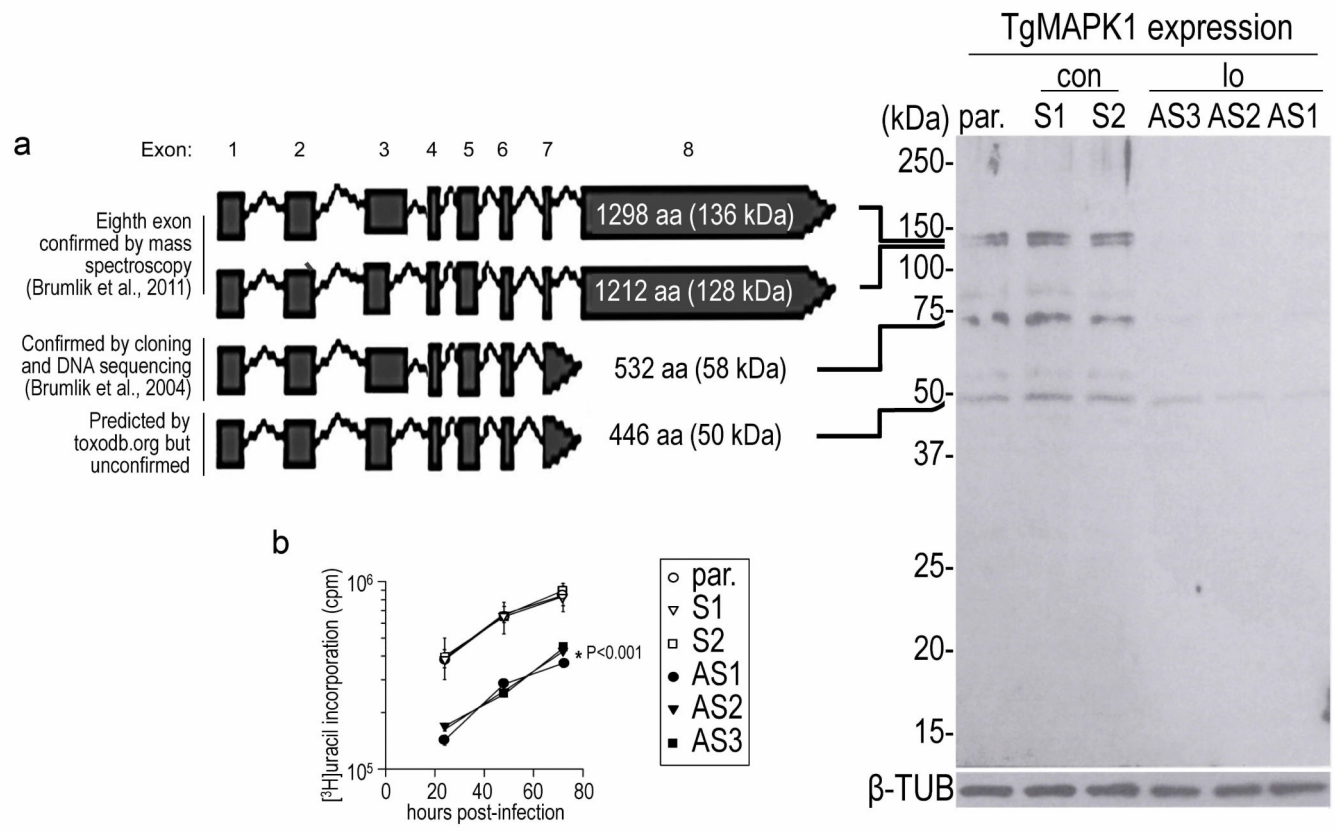

Fig. 2.

Phenotypic analysis of TgMAPK1^{con} (con) or TgMAPK1^{lo} (lo) tachyzoites. (a) human foreskin fibroblasts were infected with either TgMAPK1^{con} (con) or TgMAPK1^{lo} (lo) tachyzoites at a multiplicity of infection of 0.3. Intracellular tachyzoites were harvested seventy-two hours post-infection. Sodium dodecyl sulfate polyacrylamide gel electrophoresis and Western blotting was performed on 10^7 tachyzoites, and TgMAPK1 was detected using a rabbit anti-TgMAPK1 antibody. *T. gondii* β-tubulin served as the loading control. (b) Tachyzoite growth in human foreskin fibroblasts was assessed in triplicate by [^{3}H]uracil incorporation as a function of time.

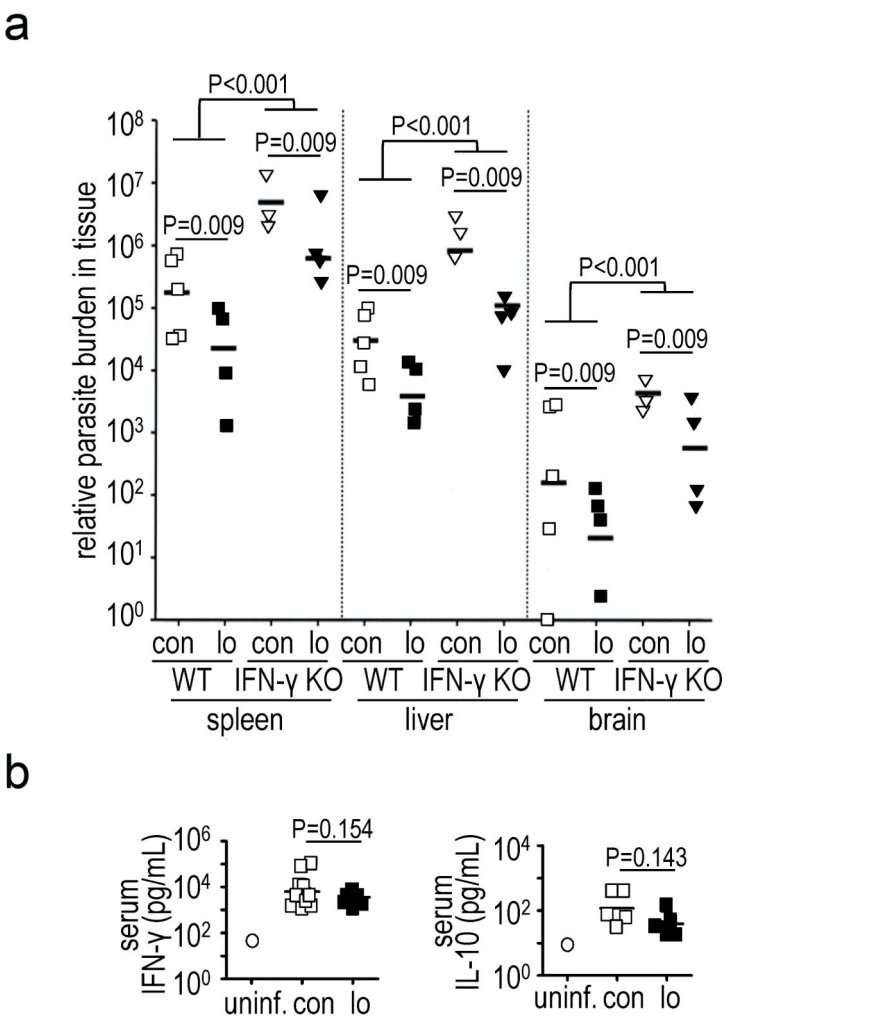

Fig. 3.

Reduced TgMAPK1 expression decreases parasite tissue burden independent of serum IFN-γ; (a) WT (*n*=10) or IFN-γ KO (*n*=5) mice were challenged intraperitoneally with 1,000 $TgMAPK1^{con}$ (con) or $TgMAPK1^{lo}$ (lo) tachyzoites and sacrificed one week later. Parasite burden by qPCR was compared using mixed-effects methods with the R package “nlme” (Pinheiro et al., 2008) adjusted for variations; (b) serum IFN-γ and IL-10 from mice in panel (a). Control serum from a naïve (uninf.) mouse is shown for comparison. Symbols represent individual mice.

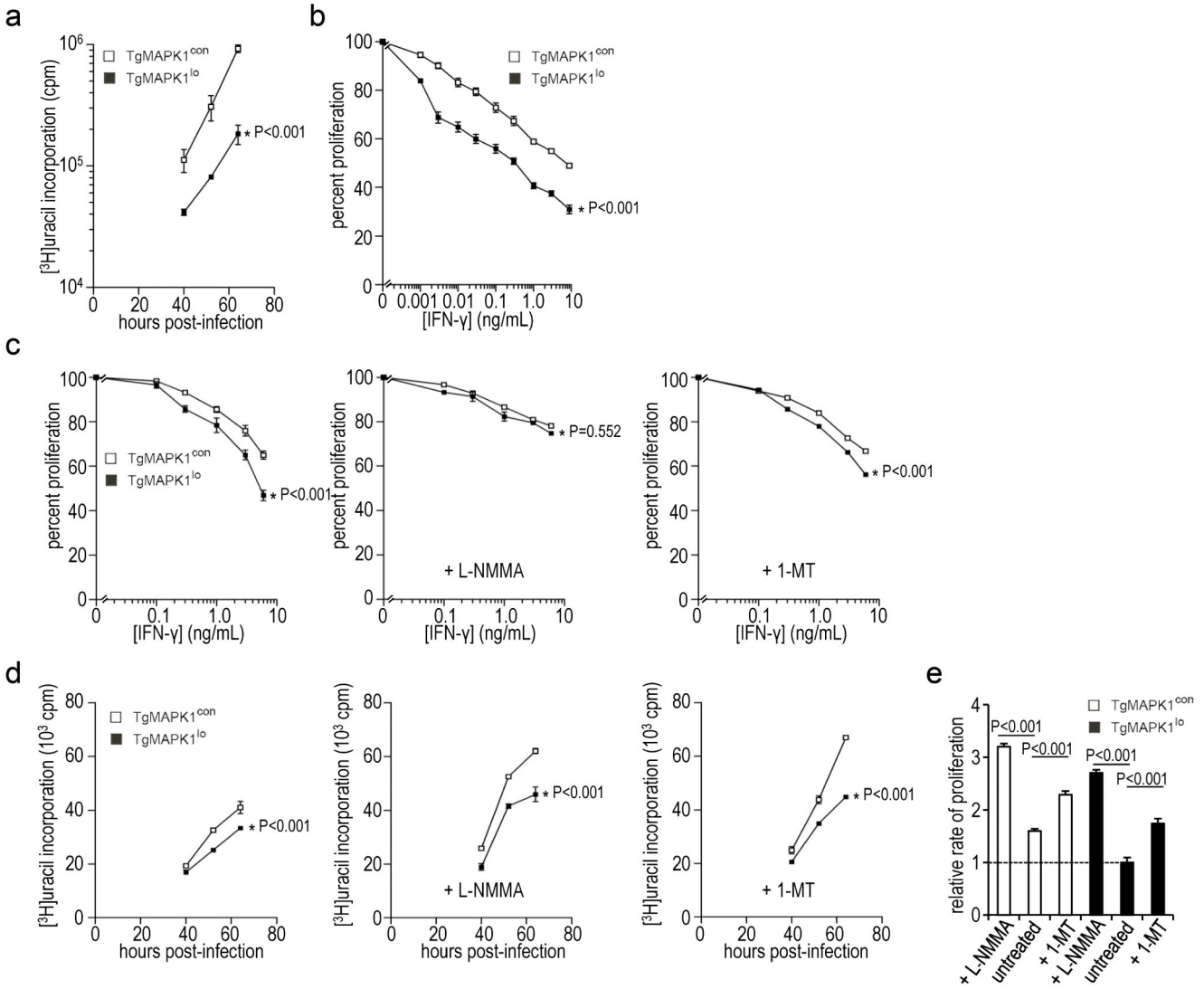

Fig. 4.

IFN-γ differentially regulates proliferation of TgMAPK1^{lo} versus TgMAPK1^{con} tachyzoites *in vitro* through an NO-dependent, IDO-independent mechanism. Mouse macrophages were infected with TgMAPK1^{con} (con) or TgMAPK1^{lo} (lo) tachyzoites at a multiplicity of infection (MOI) of 0.3. Tachyzoite proliferation was assessed in triplicate by [^{3}H]uracil incorporation. 100% proliferation represents [^{3}H]uracil incorporation without exogenous IFN-γ. One representative experiment of 2 – 4 experiments with similar results is shown; (a) tachyzoite proliferation in bone marrow-derived macrophages (BMDM) in the absence of exogenous IFN-γ as a function of time; (b) tachyzoite proliferation in BMDM assessed 52 h post-infection as a function of IFN-γ concentration (added 16 h post-infection). Assessments at 40 and 64 h yielded similar results (not shown); (c) tachyzoite proliferation in J774A.1 macrophages as a function of IFN-γ concentration (added 16 h post-infection). Indicated cells were treated with 1 mM N^G-monomethyl-L-arginine (L-NMMA) or 1-methyltryptophan (1-MT) two hours prior to infection. Proliferation was assessed 52 h post-infection. The mean ± standard error of the mean values is shown along with the *P* value for

differences between proliferation curves by ANOVA; (d) tachyzoite proliferation in J774A.1 macrophages in the absence of exogenous IFN-γ as a function of time; (e) means of triplicate growth velocities between 40 and 52 hours for the experiment shown in panel (d), normalized to untreated TgMAPK1^{lo} tachyzoites (relative rate of proliferation = 1). Bars are standard error of the means. Differences compared by *t*-test.

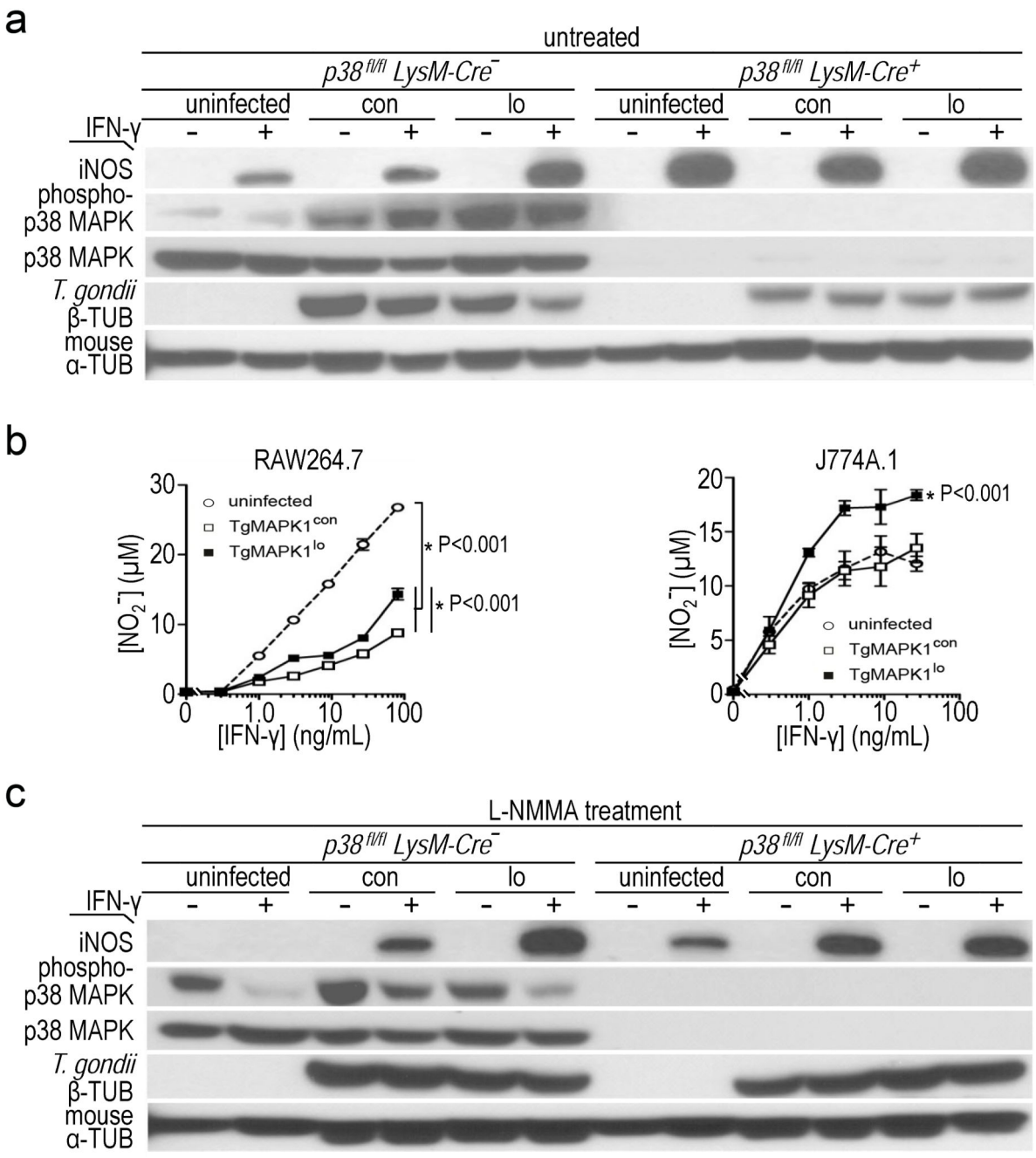

Fig. 5.

TgMAPK1-dependent IFN-γ-mediated NO regulation depends on host p38 MAPK activation; (a) bone marrow-derived macrophages (BMDM) from *p38*$^{fl/fl}$ *LysM-Cre*$^{-}$ (expressing WT p38 MAPK levels) or *p38*$^{fl/fl}$ *LysM-Cre*$^{+}$ mice (lacking p38 MAPK) were infected at a multiplicity of infection (MOI) of 0.3 with TgMAPK1^{con} (con) or TgMAPK1^{lo} (lo) tachyzoites and treated 16 h later with (+) or without (−) IFN-γ (3 ng/mL). Western blotting and enhanced chemiluminescence was performed 52 h post-infection, with one of two representative experiments being shown. Mouse α-tubulin (α-TUB) expression served

as loading control. *T. gondii* proliferation was assessed by β-tubulin (β-TUB) expression. Densitometric ratios showing phospho-p38 induction (p-p38/total p38) and tachyzoite proliferation (*T. gondii* β-TUB/mouse α-TUB) are shown in Table 1; (b) RAW264.7 or J774A.1 macrophages were infected at an MOI of 0.3 and treated with IFN-γ 16 h later. NO was measured 52 h post-infection. The *P* value for comparison of curves by ANOVA is shown with the mean ± standard error of the mean; (c) BMDM from $p38^{fl/fl}$ *LysM-Cre*$^{-}$ or $p38^{fl/fl}$ *LysM-Cre*$^{+}$ mice were treated with 1 mM N^{G}-monomethyl-L-arginine (L-NMMA) two hours before being infected, and analyzed as described in panel (a). Densitometric ratios showing phospho-p38 induction (p-p38/total p38) and tachyzoite proliferation (*T. gondii* β-TUB/mouse α-TUB) are shown in Table 2.

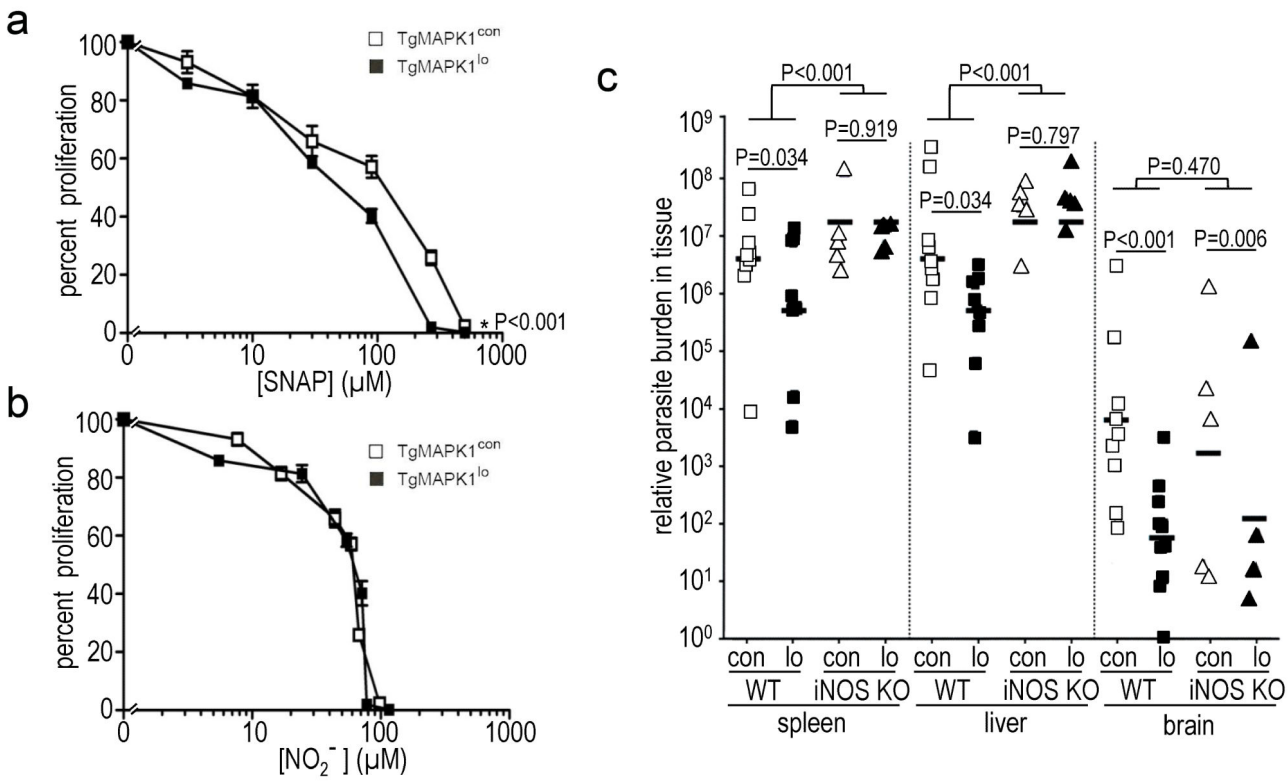

Fig. 6.

TgMAPK1 affects NO concentration without sensitizing tachyzoites to NO and iNOS deficiency equalizes parasite burden in tissues normally iNOS-replete; (a) bone marrow-derived macrophages (BMDM) from WT mice were infected at a multiplicity of infection (MOI) of 0.3 with TgMAPK1^{con} or TgMAPK1^{lo} tachyzoites and treated with 0 – 500 μM *S*-nitroso-*N*-acetylpenicillamine (SNAP); (a) tachyzoite proliferation by [^{3}H]uracil incorporation was assessed as a function of delivered SNAP concentration at 52 h post-infection; (b) proliferation in panel (a) versus actual [NO_2^-] in the culture supernatant. 100% proliferation represents [^{3}H]uracil incorporation without SNAP. Means ± standard error of the means from triplicate determinations is shown. *P* values are comparisons of curves by ANOVA; (c) WT (*n*=9-10) or iNOS KO (*n*=5) mice were challenged with 1,000 TgMAPK1^{con} (con) or TgMAPK1^{lo} (lo) and sacrificed one week later. Parasite burden by qPCR was compared using mixed-effects methods with the R package “nlme” (Pinheiro et al., 2008) adjusted for variations. Symbols represent individual mice.

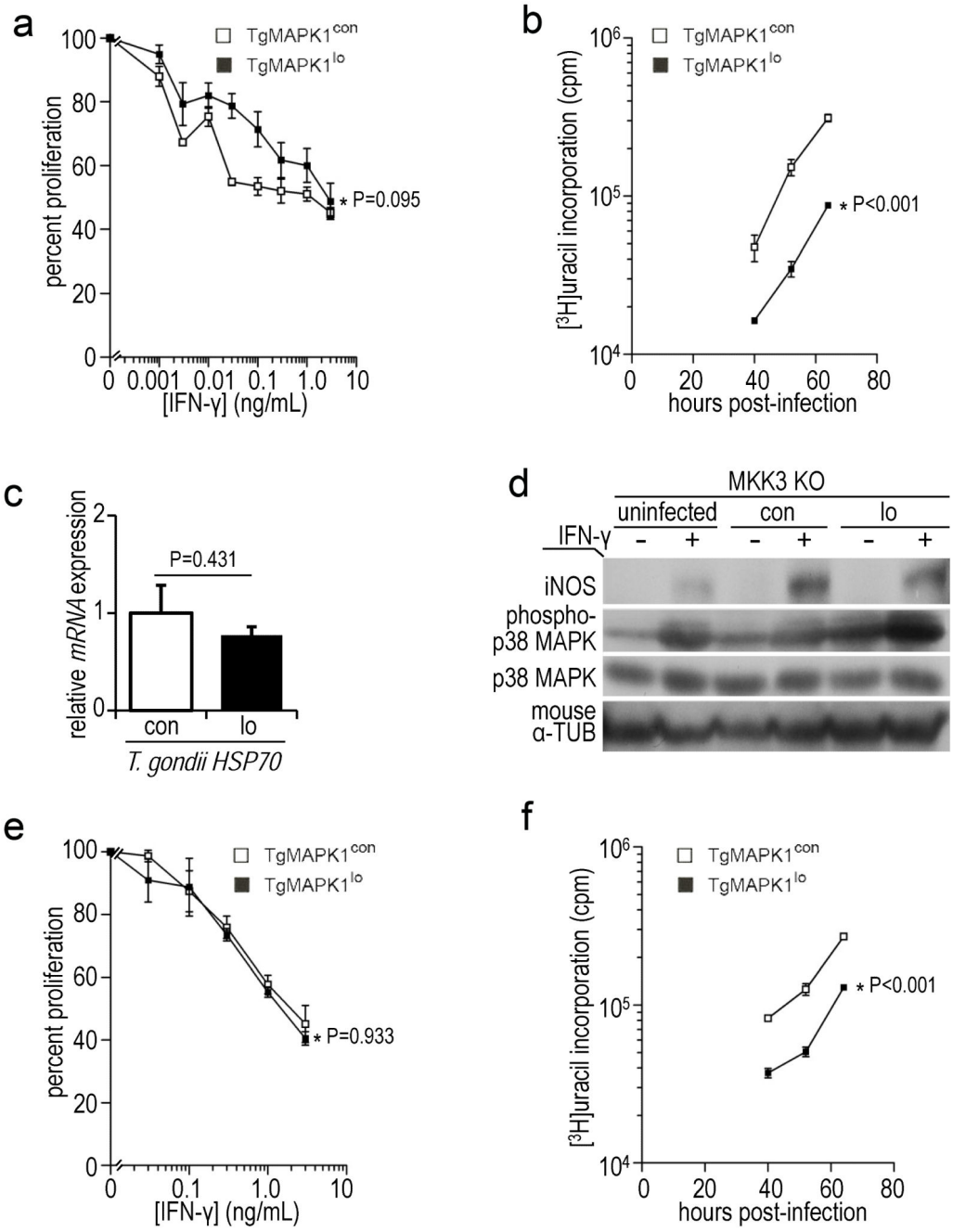

Fig. 7.

TgMAPK1-mediated control of parasite proliferation is iNOS and MKK3-dependent; (a) bone marrow-derived macrophages (BMDM) from iNOS KO mice were infected with tachyzoites at a multiplicity of infection (MOI) of 0.3 and treated with IFN-γ 16 h later. Proliferation was assessed 52 h post-infection by [^{3}H]uracil incorporation as a function of IFN-γ concentration. 100% proliferation represents [^{3}H]uracil incorporation in the absence of IFN-γ. *P* value compares curves by ANOVA; (b) proliferation in the absence of exogenous IFN-γ over time. Means ± standard error of the means is shown. *P* value

compares curves by ANOVA; (c) BMDM were infected with yellow fluorescent protein $(YFP)^+$ $TgMAPK1^{con}$ (con) or $TgMAPK1^{lo}$ (lo) tachyzoites at a MOI of 0.3. $CD11b^+YFP^+$ (infected) cells were sorted 52 h post-infection, total RNA isolated, and quantitative RT-PCR for *T. gondii HSP70* was performed, normalized to *T. gondii GAPDH*. The mean ± standard error of the mean is shown along with the *P* value (Student's *t*-test); (d) BMDM from MKK3 KO mice were infected, treated, analyzed and presented as described in Fig. 5a, along with the densitometric ratios showing phospho-p38 induction (p-p38/total p38) in Table 3; (e) MKK3 KO BMDM were infected and treated with IFN-γ as described in panel (a); (f) proliferation in panel (e) in the absence of exogenous IFN-γ over time. Mean of triplicates ± standard errors of the mean is shown and *P* values compare curves by ANOVA.

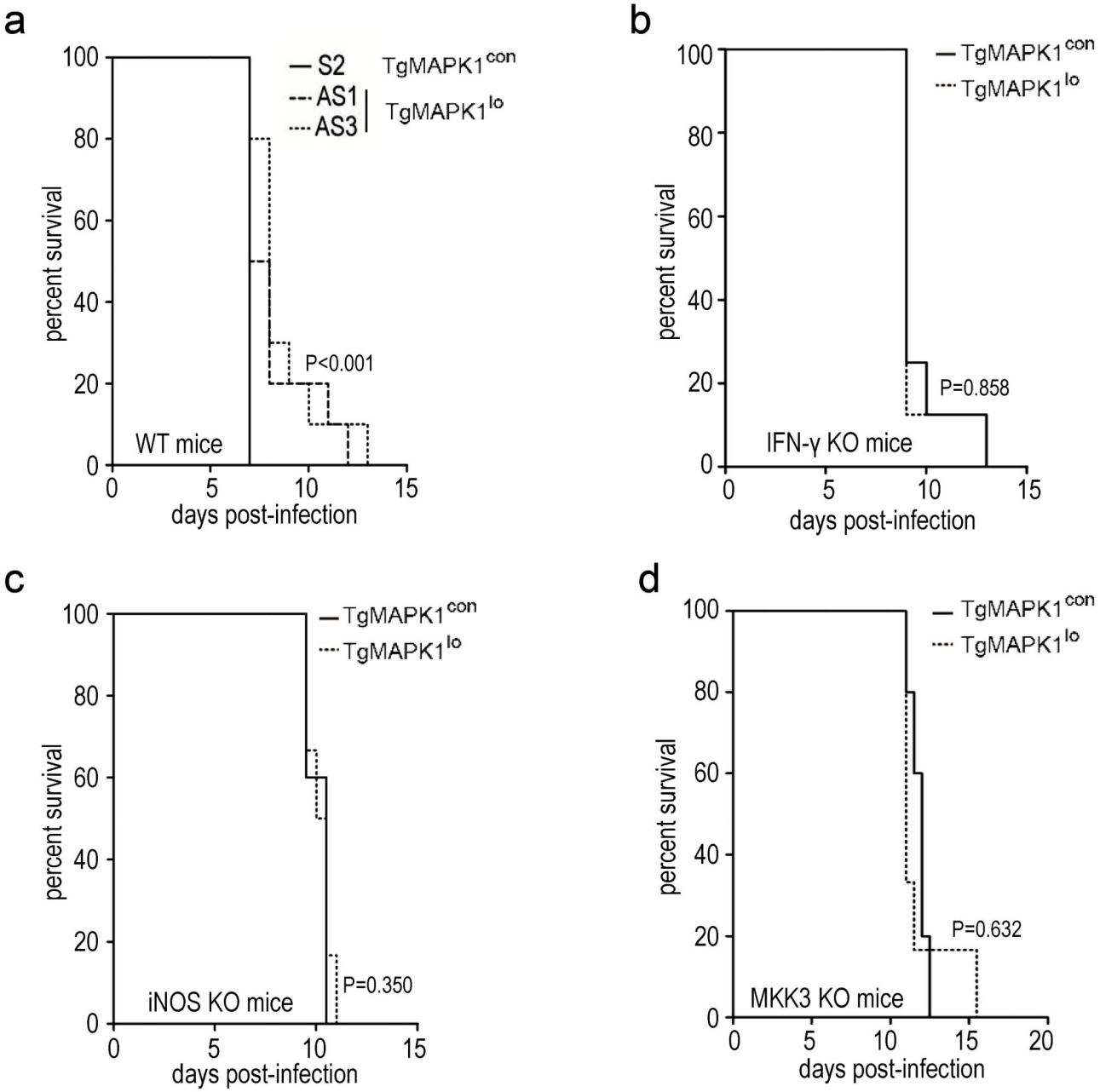

Fig. 8.

TgMAPK1-dependent virulence is IFN-γ, iNOS, and MKK3-dependent; (a) WT mice (*n*=10) were challenged with 50,000 TgMAPK1^{con} or TgMAPK1^{lo} tachyzoites and survival was assessed by the Kaplan-Meier method and compared by the log rank test. This inoculum was chosen for survival studies involving immunocompetent wild type mice because it consistently caused 100% mortality while demonstrating a significant difference between TgMAPK1^{con} or TgMAPK1^{lo} infection. Due to the fact that IFN-γ, iNOS, and MKK3 KO mice were highly susceptible to *T. gondii* infection, IFN-γ KO (*n*=8) (b), iNOS KO (*n*=5–6) (c), or MKK3 KO (*n*=6–8) (d) mice were challenged with a much lower inoculum (10,000 tachyzoites) and survival assessed as in panel (a). For panels (b) – (d), inocula as high as

50,000 tachyzoites were also examined but this caused very rapid mortality between 6 – 8 days post-infection without demonstrating any statistically significant differences between TgMAPK1^{con} or TgMAPK1^{lo} infection (not shown).

Table 1

Densitometric ratios showing phospho-p38 induction (p-p38/total p38) and tachyzoite proliferation (*T. gondii* β-tub/mouse α-tub) in *p38$^{fl/fl}$LysM-Cre^{-}* and *p38$^{fl/fl}$LysM-Cre^{+}* BMDM.

		uninfected		**TgMAPK1^{con}**		**TgMAPK1^{lo}**	
	IFN-γ added→ genotype↓	−	+	−	+	−	+
$\frac{\text{p} - \text{p38}}{\text{total p38}}$	*p38$^{fl/fl}$LysM-Cre* $^{-}$	0.13±0.10	0.17±0.10	0.55±0.03	1.10±0.12	1.04±0.02	1.10±0.01
	p38$^{fl/fl}$LysM-Cre $^{+}$	0	0	0	0	0	0
$\frac{\beta - \text{tub}}{\alpha - \text{tub}}$	*p38$^{fl/fl}$LysM-Cre* $^{-}$	0	0	1.10±0.07	1.04±0.03	0.86±0.05	0.51±0.01
	p38$^{fl/fl}$LysM-Cre $^{+}$	0	0	0.49±0.02	0.56±0.03	0.57±0.10	0.57±0.03

Table 2

Densitometric ratios showing phospho-p38 induction (p-p38/total p38) and tachyzoite proliferation (*T. gondii* β-tub/mouse α-tub) in L-NMMA-treated *p38$^{fl/fl}$LysM-Cre^{-}* and *p38$^{fl/fl}$LysM-Cre^{+}* BMDM.

		uninfected		**TgMAPK1^{con}**		**TgMAPK1^{lo}**	
	IFN-γ added→ genotype↓	−	+	−	+	−	+
$\frac{\text{p} - \text{p38}}{\text{total p38}}$	*p38$^{fl/fl}$LysM-Cre* $^{-}$	0.62±0.12	0.13±0.07	1.17±0.08	0.70±0.19	0.70±0.19	0.31±0.07
	p38$^{fl/fl}$LysM-Cre $^{+}$	0	0	0	0	0	0
$\frac{\beta - \text{tub}}{\alpha - \text{tub}}$	*p38$^{fl/fl}$LysM-Cre* $^{-}$	0	0	1.02±0.06	1.00±0.05	0.87±0.02	0.82±0.05
	p38$^{fl/fl}$LysM-Cre $^{+}$	0	0	0.78±0.03	0.92±0.09	1.02±0.09	1.19±0.17

Table 3

Densitometric ratios showing phospho-p38 induction (p-p38/total p38) in MKK3 KO BMDM.

	uninfected		**TgMAPK1^{con}**		**TgMAPK1^{lo}**	
IFN-γ added→	−	+	−	+	−	+
$\frac{\text{p − p38}}{\text{total p38}}$	0.09±0.07	0.57±0.12	0.24±0.07	0.46±0.11	0.54±0.13	1.02+0.01